Planetary and Space Science 261 (2025) 106102

Contents lists available at ScienceDirect

Planetary and Space Science

journal homepage: www.elsevier.com/locate/pss

Short communication

Pre-perihelion observations of the carbon-depleted comet C/2023 A3 (Tsuchinshan-ATLAS). Insights into CN production and molecular upper limits

Pamela Cambianica [a,*], Giovanni Munaretto [a], Gabriele Cremonese [a], Alessandra Mura [a,b], Fiorangela La Forgia [b], Luca Bizzocchi [c], Monica Lazzarin [b], Cristina Puzzarini [c], Mattia Melosso [c], Vania Lorenzi [d,e], Walter Boschin [d,e,f]

[a] INAF Astronomical observatory of Padova, vicolo dell'Osservatorio 5, 35122, Padova, Italy
[b] Department of Physics and Astronomy "Galileo Galilei", University of Padova, Vicolo dell'Osservatorio 3, 35122, Padova, Italy
[c] Department of Chemistry "Giacomo Ciamician", University of Bologna, Via F. Selmi 2, 40126, Bologna, Italy
[d] Fundación Galileo Galilei-INAF, Rambla José Ana Fernandez Pérez 7, 38712, Breña Baja, TF, Spain
[e] Instituto de Astrofisica de Canarias, C/Via Lactea s/n, 38205, La Laguna, Tenerife, Spain
[f] Departamento de Astrofisica, Univ. de La Laguna, Av. del Astrofisico Francisco Sánchez s/n, 38205, La Laguna, Tenerife, Spain

ARTICLE INFO

Keywords:
Comets
General – instrumentation
Spectrographs – methods
Data analysis

ABSTRACT

The study of cometary molecular emissions provides crucial insights into the primordial composition of the Solar System and the physical and chemical processes shaping these icy bodies. Comets, as remnants of the early Solar System, serve as natural archives of volatile compounds that offer a glimpse into the conditions of the protoplanetary disk. In this work, we analyze an optical pre-perihelion spectrum of comet C/2023 A3 (Tsuchinshan-ATLAS), obtained using the DOLORES spectrograph at the Telescopio Nazionale Galileo (TNG) on May 1, 2024. The cometary spectrum was reduced using standard procedures implemented in the IRAF software package. To characterize the volatile inventory of comet C/2023 A3, we derived the production rate of CN, the only detectable molecular emission, and calculated upper limits for undetected species, including C_2, C_3, and NH_2. These constraints were obtained by analyzing the noise level in continuum regions and integrating theoretical line profiles, accounting for instrumental resolution and observational conditions. We calculated a CN production rate of $(3.89\pm0.21)\times10^{25}$ molec/s. Despite significant dust contamination, which likely obscures weaker molecular emission lines typically associated with cometary activity, we derived upper limits for the production rates of key volatile species: $Q_{C_3} < 3.12\times10^{24}$ molec/s, $Q_{C_2} < 1.30\times10^{25}$ molec/s, and $Q_{NH_2} < 2.79\times10^{25}$ molec/s, respectively. We also determined the $Af\rho$ parameter, obtaining a value of 4329 ± 56 cm, which confirms the high dust production rate previously reported for this comet. The logarithmic ratio of production rates, $\log\left(Q(C_2)/Q(CN)\right) < -0.48$, indicates that C/2023 A3 is a carbon-depleted comet, consistent with previous classifications of dynamically new comets. These findings contribute to a deeper understanding of the compositional diversity and evolutionary processes of such objects.

1. Introduction

Comets are among the most pristine remnants of the early Solar System, preserving the primordial materials that contributed to the formation of the Sun and planets (Morbidelli and Rickman, 2015). Composed primarily of volatile ices, refractory dust, and organic compounds, comets offer a unique opportunity to investigate the conditions and composition of the protoplanetary disk (Russo et al., 2016; Mumma and Charnley, 2011; Lippi et al., 2024). When they approach the Sun, sublimation processes result in the release of gas and dust that form a coma and tails. These features make comets invaluable for studying the chemical and physical evolution of Solar System bodies. The molecular species observed in the comae of comets provide key insights into their volatile inventories and photochemical processes. These species are both parent volatiles that sublimate from the nucleus and daughter species produced through the photodissociation of these parent volatiles in the coma. Understanding the abundances of these

* Corresponding author.
E-mail address: pamela.cambianica@inaf.it (P. Cambianica).

https://doi.org/10.1016/j.pss.2025.106102
Received 19 December 2024; Received in revised form 19 March 2025; Accepted 21 March 2025
Available online 3 April 2025

Table 1
Observing parameters at the moment of observations. The heliocentric distance, Right Ascension (RA), Declination (DEC), the geocentric distance (Δ), the geocentric velocity ($\dot{\Delta}$), the exposure time, and the airmass are reported.

Date	Heliocentric distance	RA	DEC	Δ	$\dot{\Delta}$	Exposure time	Airmass
	AU	HH MM SS.ff	sDD-MN-SC.f	AU	km/s	s	
01-05-2024	2.76	13 22 48.42	−00 50 19.9	1.81	−12.32	300	1.15

molecules not only aids in reconstructing the volatile composition of comets but also provides critical information about the chemical pathways operating in their comae (Biver et al., 2024).

Discovered by the Tsuchinshan Observatory and the ATLAS survey on January 9, 2023, the dynamically new comet C/2023 A3 (Tsuchinshan-ATLAS) reached its perihelion on September 27, 2024, at a distance of 0.391 au from the Sun. As C/2023 A3 approached the inner Solar System and perihelion, its activity increased significantly, with a substantial production of dust (Mugrauer, 2024). While such dust activity contributes to the striking visual features often associated with comets, it also poses substantial challenges for detailed spectroscopic analyses. The strong dust continuum observed in comet C/2023 A3 significantly impacts the detectability of weak molecular emission features. The intense background continuum lowers the signal-to-noise ratio, making it challenging to distinguish faint lines such as C_2, C_3, and NH_2 from spectral noise. Additionally, dust scattering can dilute intrinsic molecular emissions, reducing their observed intensity. While a solar analog star was used to model and subtract the dust continuum, variations in dust reflectance properties and broad-band spectral residuals may still obscure weak emission bands. These factors contribute to the stringent upper limits derived for undetected molecular species in this study.

In this work, we analyze an optical spectrum of comet C/2023 A3 obtained with the DOLORES spectrograph at the Telescopio Nazionale Galileo (TNG) on May 1, 2024, calculating the production rate of CN, deriving upper limits for the production rates of key molecular species, and comparing them with those of other comets reported in the literature.

2. Observations and data reduction

The observation of comet C/2023 A3 was conducted using the DOLORES (Device Optimized for the LOw RESolution) spectrograph mounted on the 3.58 m Telescopio Nazionale Galileo (TNG). For this study, the LR-B grism was employed in combination with a 1.0" slit width, providing a spectral resolution of $R = \lambda/\Delta\lambda = 600$, sufficient to resolve key molecular emission features typically observed in cometary spectra. The spectrum was obtained on May 1, 2024. Table 1 shows the observing circumstances at the moment of observations. The cometary spectra (see Fig. 1) were reduced using standard procedures implemented in the IRAF (Tody, 1986) software package, following the classical extraction method by Horne (1986). The reduction process included bias subtraction (the bias is computed on the over-scan regions of the frame), flat-field correction, and wavelength calibration. Wavelength calibration was performed using comparison spectra from He and Ne+Hg lamps. Subsequently, the spectra were flux-calibrated using observations of a spectrophotometric standard star (SA 107–684). To isolate the molecular emission features and remove the continuum contribution from dust, we used the solar analog star Land102-1081. The calibration accounted for instrumental response and atmospheric extinction, ensuring the spectra were suitable for quantitative analysis of the cometary emissions (see Fig. 2).

3. Methods

To characterize the volatile content of comet C/2023 A3, we analyzed the obtained spectrum to determine the CN production rate, the only molecular emission detected, and to establish upper limits for undetected species, including C_2, C_3, and NH_2. The following sections detail the methods employed for these analyses.

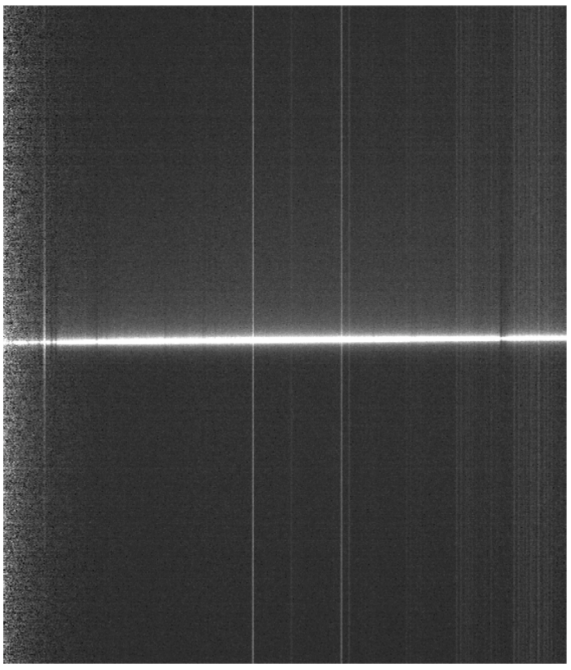

Fig. 1. 2D-emission spectrum of comet C/2023 A3 (Tsuchinshan-ATLAS). The spectrum refers to 1 May, 2024.

3.1. Determination of the CN production rate

The production rate of CN (B-X) was derived by analyzing its emission band centered at 3883 Å. The integrated flux of the emission, $F_{\rm obs}$, was measured in IRAF through a fit of a Gaussian profile, centered at the catalog wavelength (see Fig. 3). The spatial distribution of CN emission along the slit was modeled using the Haser model (Haser, 1957), which assumes isotropic expansion of the molecules in the coma. To convert the observed flux into a production rate, we applied the method by Fink and Hicks (1996), which is given by:

$$Q = \frac{4\pi\Delta^2 V_{out}}{g\beta_d} \cdot F_{obs} \cdot H, \quad (1)$$

where Δ is the geocentric distance, V_{out} is the outflow velocity of molecules in the coma (Faggi et al., 2021; Rauer et al., 2003), g is the fluorescence efficiency (i.e., g-factor) of the molecule, and β_d is the molecule's daughter scale length. F_{obs} is the flux emitted by the molecule, and H is the Haser correction. The uncertainty on the outflow velocity (V_{out}) was estimated based on empirical variations observed in previous studies (e.g., (A'Hearn et al., 1995; Biver et al., 2024)), and given the lack of direct measurements and for consistency with previous works, we assumed the same outflow velocity for all molecular species, scaled according to the heliocentric distance. In the Haser model calculation, molecular g−factor, scale length and their errors were taken from (Fink and Hicks, 1996; Langland-Shula and Smith, 2011; Meier et al., 1998; Schleicher, 2009). The Haser model parameters, including the scale lengths, were optimized to match the observed flux distribution along the long slit, following the methodology described by Fray et al. (2005) (see Table 2). This approach ensures that the derived production rate is consistent with the spatial

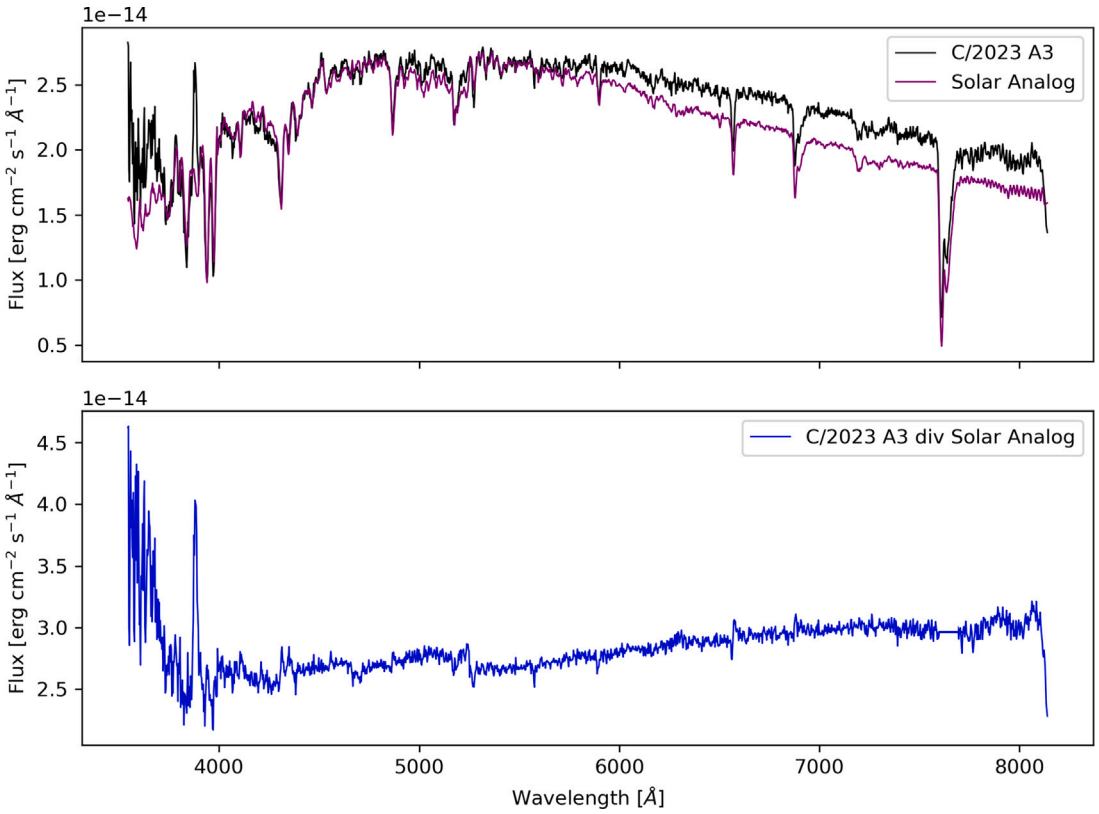

Fig. 2. 1D-emission spectrum of comet C/2023 A3 (Tsuchinshan-ATLAS). Spectral range: 350–820 nm. The spectrum refers to 1 May, 2024. Top panel: Comparison between the observed spectrum of comet C/2023 A3 (black) and the solar analog spectrum (purple). Bottom panel: The spectrum of C/2023 A3 after division by the solar analog.

Table 2
Parameters and production rates used to determine the molecular abundances in comet C/2023 A3. V_{out} is the gas outflow velocity, g is the molecular g-factor, β_d is the daughter scale length, and F_{obs} is the observed flux. The production rates and corresponding mixing ratios are shown in the last two columns. Values are scaled to the heliocentric distance of the observation.

Molecule	V_{out}	g	β_d	F_{obs}	Production Rate	log[Q(X)/Q(CN)]
		10^{-14}	10^5	10^{-13}		
	km s^{-1}	erg s^{-1} mol^{-1}	km	erg cm^{-2} s^{-1}	molec/s	
CN	0.48 ± 0.12	3.99	6.9	3.45	$(3.89 \pm 0.21) \times 10^{25}$	–
C_2	"	5.91	1.7	–	$< 1.30 \times 10^{25}$	< -0.48
C_3	"	13.10	61.2	–	$< 3.12 \times 10^{24}$	< -1.10
NH_2	"	1.03	4.58	–	$< 2.79 \times 10^{25}$	< -0.14

emission profile. Errors in the model parameters, including the observed flux, the scale lengths and outflow velocity, were propagated to estimate the uncertainty in the production scale calculation, as shown in Langland-Shula and Smith (2011).

3.2. Upper limits for other molecular species

We looked for the C_2 (0–0) emission band near 516.7 nm, which is typically the second most prominent species in the optical spectrum of comets, but it was not detected. No emission from C_3 (A–X) band around 405 nm, or the main NH_2 (0–0) band centered around 553 nm could be detected either (see Fig. 4). For undetected molecular species, upper limits were derived based on the noise level in the spectrum at the wavelengths corresponding to their expected emissions. The root mean square (RMS) of the continuum flux, σ_{cont}, was calculated around the wavelengths of C_2, C_3, and NH_2. This RMS was taken as the 1σ threshold for undetected lines. The upper limit for the flux, F_{lim}, was approximated as:

$$F_{\text{lim}} = 3\sigma_{\text{cont}} \Delta\lambda, \tag{2}$$

where $\Delta\lambda$ represents the width of the expected molecular band. The upper limit fluxes were then converted into production rates using the same formalism described for CN, substituting the appropriate g–factors for C_2, C_3, and NH_2 using a Haser model as mentioned above (see Table 2). The upper limit production rates were calculated assuming the same expansion velocity as for CN, ensuring consistency in the coma model. These upper limits provide constraints on the maximum abundance of the undetected species under the observational conditions.

3.3. Baseline determination and uncertainty estimation

The determination of the spectral baseline in comet C/2023 A3 (Tsuchinshan-ATLAS) presented a particular challenge due to the strong dust continuum, which significantly contaminated the spectrum and obscured weaker molecular emission features. To address this, we adopted a two-step method:

1. Continuum fitting: we fitted the continuum using a low-order polynomial function applied to regions of the spectrum free from known molecular emissions. These regions were carefully selected to avoid contamination from prominent emission features such as CN, C_2, C_3, and NH_2. The fit was performed iteratively, minimizing the residuals between the observed spectrum and

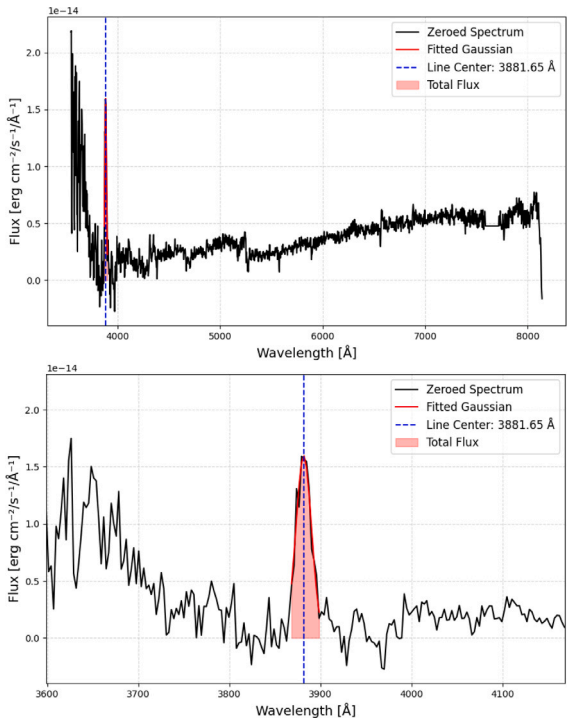

Fig. 3. *Top panel*. Gaussian fit to the CN emission band centered at 3881.68 Å in the comet's spectrum. The black line represents the observed spectrum, the red line is the fitted Gaussian profile, the blue dashed line indicates the central wavelength, and the shaded area corresponds to the total flux under the curve. *Bottom panel*. Zoomed-in view of the CN emission band and its Gaussian fit. The detailed view highlights the agreement between the fitted Gaussian profile (red line) and the observed data (black line), with the shaded area representing the integrated flux. The central wavelength is marked by the blue dashed line.

the fitted model to ensure an accurate representation of the underlying dust contribution.

2. Solar analog subtraction: to account for the reflected solar contribution from dust particles, we subtracted a scaled spectrum of a solar analog star observed with the same instrumental setup.

The uncertainties in the baseline determination were estimated by analyzing the root-mean-square (RMS) fluctuations in regions of the spectrum free from molecular emissions.

4. Results and conclusions

4.1. Determination of production rates and mixing ratios

The production rate of CN was determined to be $(3.89 \pm 0.21) \times 10^{25}$ molec/s. This value reflects the significant presence of CN in the comet's coma, making it the dominant detectable molecular species in our observations. The derived upper limits for C_2, C_3, and NH_2 are: $Q_{C_3} < 3.12 \times 10^{24}$ molec/s, $Q_{C_2} < 1.30 \times 10^{25}$ molec/s, and $Q_{NH_2} < 2.79 \times 10^{25}$ molec/s. The results underscore the dominance of CN in the volatile inventory of comet C/2023 A3, as it is the only species detected with a production rate well above the derived upper limits of the other molecules. These findings contribute to a better understanding of the molecular composition and photochemical processes in the coma of comets, particularly those with significant dust contamination that can obscure fainter emissions. A comparison with the results reported by Ahuja et al. (2024) reveals some differences. Ahuja et al. (2024) measured a CN production rate of $(4.73 \pm 0.23) \times 10^{25}$ molec/s, slightly higher than our measurement. Additionally, they derived upper limits for C_2, C_3, and NH_2 that are comparable to ours: $Q_{C_2} < 1.49 \times 10^{25}$ molec/s, $Q_{C_3} < 3.36 \times 10^{24}$ molec/s, and $Q_{NH_2} < 2.95 \times 10^{25}$ molec/s.

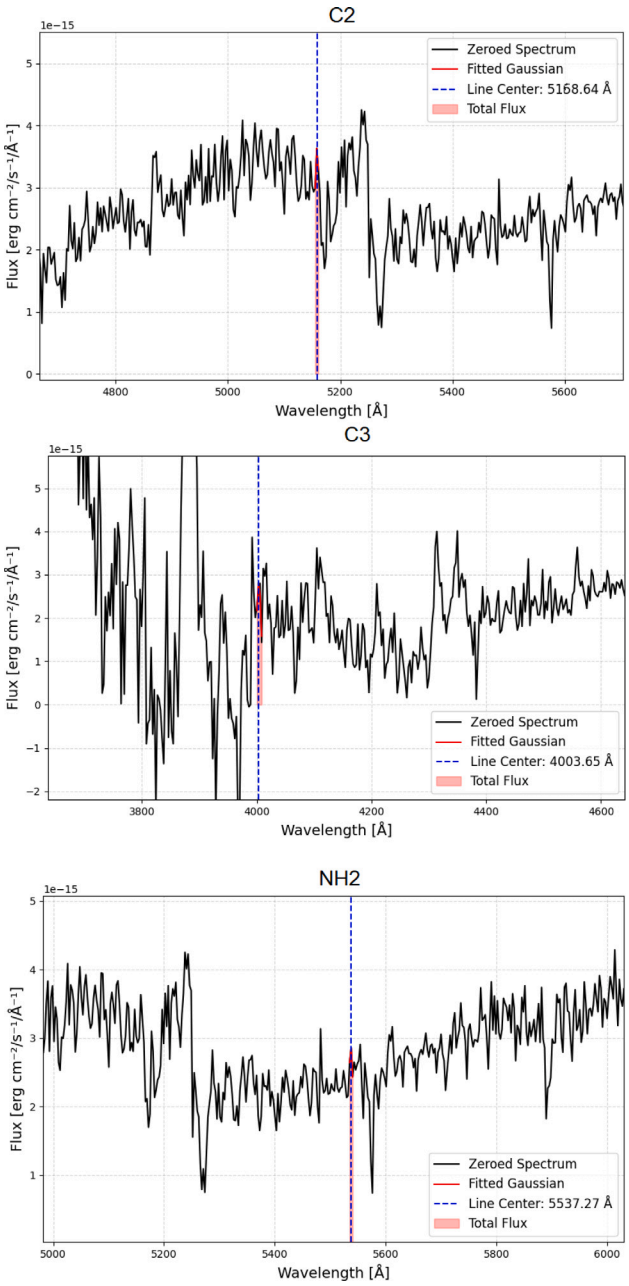

Fig. 4. *Top panel*: Observed spectrum of comet C/2023 A3 in the spectral region of the C_2 bandhead at 5168.64 Å. The black line represents the observed spectrum, while the blue dashed line marks the expected central wavelength of the molecular feature. The shaded red region indicates the area where the emission would be expected, but no significant detection is observed. *Middle panel*: Same as the top panel but for the C_3 bandhead at 4003.65 Å. *Bottom panel*: Same as the previous panels but for the NH_2 bandhead at 5537.27 Å.

Furthermore, Jehin et al. (2024) reported a CN production rate of $(5.39 \pm 0.52) \times 10^{25}$ molec/s, which is higher than both our measurement and that of Ahuja et al. (2024). Notably, Jehin et al. (2024) also detected C_2 with a production rate of $(1.66 \pm 0.42) \times 10^{25}$ molec/s, whereas in our observations and those of Ahuja et al. (2024), C_2 was not detected, and upper limits were established. Jehin et al. (2024) reported a $\log(Q(C_2)/Q(CN))$ ratio of -0.58 ± 0.15, indicating a carbon-chain depleted composition. These discrepancies could be attributed to several factors, including differences instrumentation sensitivity, or the comet's activity levels at the times of observation. Our observations were conducted on May 1, 2024, at a heliocentric distance of 2.76 AU,

while (Ahuja et al., 2024)'s observations took place on May 31, 2024, at 2.33 AU, and Jehin et al. (2024)'s on July 4, 2024, at 1.81 AU. The closer proximity to the Sun in the latter observations could have resulted in increased sublimation rates, leading to higher production rates of volatile species.

We now proceed to compare our results with those reported for other comets to assess whether all comets share a similar composition or if fundamental differences exist. Should such differences be identified, further questions arise regarding their origin, whether they result from distinct formation environments or divergent evolutionary processes. We compared our derived production rate ratios for comet C/2023 A3 with those reported in the literature (A'Hearn et al., 1995; Fink, 2009; Cochran et al., 2012). Our measured values are $\log[Q(C_2)/Q(\mathrm{CN})] < -0.48$, $\log[Q(C_3)/Q(\mathrm{CN})] < -1.10$, and $\log[Q(NH_2)/Q(\mathrm{CN})] < -0.14$. These values are all lower than the average values observed in typical comets, which are 0.15 ± 0.20, -0.68 ± 0.20, and -0.09 ± 0.27 for C_2, C_3, and NH_2, respectively. According to the carbon-depletion classification criteria, the ratio of -1.10 for C_3 and -0.48 for C_2 indicate that the comet can be classified as carbon-depleted according to the definitions provided in previous studies (e.g., (Cochran et al., 2012)). The $\log[Q(NH_2)/Q(CN)] < -0.14$ ratio, although slightly below the average value for typical comets, does not significantly deviate from the expected range for non-depleted comets. These results suggest that C/2023 A3 exhibits a clear carbon-chain depletion pattern, which could be indicative of intrinsic compositional differences or the result of evolutionary processes affecting its volatile inventory.

4.2. Determination of $Af\rho$ and dust production analysis

The dust production rate of comet C/2023 A3 was quantified using the $Af\rho$ parameter, following the method described by A'Hearn et al. (1995). In our observations, we derived an $Af\rho$ value of 4329 ± 56 cm at a heliocentric distance of $r_h = 2.76$ au and a geocentric distance of $\Delta = 1.5$ au. The uncertainty on the $Af\rho$ parameter was estimated by propagating the individual errors on the heliocentric distance (r_h), geocentric distance (Δ), observed cometary flux, and solar analog flux. This calculation was performed using standard error propagation techniques, taking into account the contributions from both observational uncertainties and geometric parameters. This value reflects the comet's significant dust production activity during our observation window. Our $Af\rho$ measurement is comparable to values reported in previous studies. Specifically, observations from July 4, 2024, reported $Af\rho$ values of 6007 ± 68 cm (Jehin et al., 2024). These observations were taken at $r_h = 1.81$ au and $\Delta = 1.99$ au. Although our measurement is slightly lower, this discrepancy can be attributed to the larger heliocentric distance during our observation, as dust production typically increases with decreasing r_h.

A further point of comparison concerns the comet's dust-to-gas ratio. Previous reports measured a dust-to-gas ratio of $\log(Af\rho/Q(CN)) = -21.94 \pm 0.04$. Our calculated ratio of $\log(Af\rho/Q(CN)) = -21.87 \pm 0.03$ (assuming $Q(CN) = (3.89 \pm 0.21) \times 10^{25}$ molec/s) is consistent with these earlier findings.

The comparison between our measurements and previous observations highlights both the temporal evolution of C/2023 A3's dust production and the consistency of its carbon-chain depletion. The observed increase in dust activity aligns with trends seen in other observations closer to the comet's perihelion, while the stable dust-to-gas ratio suggests persistent compositional characteristics over time. These findings contribute to the broader understanding of the physical and chemical evolution of dynamically new comets from the Oort Cloud.

CRediT authorship contribution statement

Pamela Cambianica: Writing – original draft, Methodology, Data curation, Conceptualization. **Giovanni Munaretto:** Writing – review & editing, Methodology, Conceptualization. **Gabriele Cremonese:** Writing – review & editing, Supervision, Funding acquisition, Conceptualization. **Alessandra Mura:** Methodology, Formal analysis. **Fiorangela La Forgia:** Writing – review & editing, Supervision, Methodology. **Luca Bizzocchi:** Writing – review & editing, Supervision. **Monica Lazzarin:** Writing – review & editing, Supervision, Methodology. **Cristina Puzzarini:** Writing – review & editing. **Mattia Melosso:** Writing – review & editing. **Vania Lorenzi:** Writing – review & editing, Data curation. **Walter Boschin:** Writing – review & editing, Data curation.

Declaration of competing interest

The authors declare that they have no known competing financial interests or personal relationships that could have appeared to influence the work reported in this paper.

Acknowledgments

This research used the facilities of the Italian Center for Astronomical Archive (IA2) operated by INAF at the Astronomical Observatory of Trieste.

Data availability

Data will be made available on request.

References

A'Hearn, M.F., Millis, R.C., Schleicher, D.G., Osip, D.J., Birch, P.V., 1995. The ensemble properties of comets: results from narrowband photometry of 85 comets, 1976-1992. Icarus 118 (2), 223–270.

Ahuja, G., Aravind, K., Sahu, D., Jehin, E., Donckt, M.V., Hmiddouch, S., Ganesh, S., Sivarani, T., 2024. Molecular gas production rates of Comet C/2023 A3 (Tsuchinshan-ATLAS). In: The Astronomer's Telegram. p. 16637.

Biver, N., Bockelée-Morvan, D., Handzlik, B., et al., 2024. Chemical composition of comets C/2021 A1 (Leonard) and C/2022 E3 (ZTF) from radio spectroscopy and the abundance of HCOOH and HNCO in comets. Astron. Astrophys. Vol. 690, A271.

Cochran, A., Barker, E.S., Gray, C.L., 2012. Thirty years of cometary spectroscopy from McDonald Observatory. Icarus 218 (1), 144–168.

Faggi, S., Lippi, M., Camarca, M., Buzard, C.F., Villanueva, G.L., Doppmann, G.W., Blake, G.A., Mumma, M.J., 2021. The extraordinary passage of Comet C/2020 F3 NEOWISE: Evidence for heterogeneous chemical inventory in its nucleus. Astron. J. 162 (5), 178.

Fink, U., 2009. A taxonomic survey of comet composition 1985–2004 using CCD spectroscopy. Icarus 201 (1), 311–334.

Fink, U., Hicks, M.D., 1996. A survey of 39 comets using CCD spectroscopy. Astrophys. J. 459, 729–743.

Fray, N., Bénilan, Y., Cottin, H., Gazeau, M.-C., Crovisier, J., 2005. The origin of the CN radical in comets: A review from observations and models. Planet. Space Sci. 53 (12), 1243–1262.

Haser, L., 1957. Distribution d'intensité dans la tête d'une comète. Bull. de L' Académie R. de Belg. 43 (1), 740–750.

Horne, K., 1986. An optimal extraction algorithm for CCD spectroscopy. Publ. Astron. Soc. Pac. 98 (604), 609.

Jehin, E., Donckt, M.V., Hmiddouch, S., Manfroid, J., 2024. TRAPPIST bright comets production rates: 13P/Olbers, C/2023 A3 (Tsuchinshan - ATLAS) and C/2021 S3 (PanSTARRS). In: The Astronomer's Telegram. p. 16705.

Langland-Shula, L.E., Smith, G.H., 2011. Comet classification with new methods for gas and dust spectroscopy. Icarus 213 (1), 280–322.

Lippi, M., Podio, L., Codella, C., Faggi, S., De Simone, M., Villanueva, G.L., Mumma, M.J., Ceccarelli, C., 2024. The ice chemistry in comets and planet-forming disks: Statistical comparison of CH_3OH, H_2CO, and NH_3 abundance ratios. Astrophys. J. Lett. 970 (1), L5.

Meier, R., Wellnitz, D., Kim, S.J., A'Hearn, M.F., 1998. The NH and CH bands of comet C/1996 B2 (Hyakutake). Icarus 136 (2), 268–279.

Morbidelli, A., Rickman, H., 2015. Comets as collisional fragments of a primordial planetesimal disk. Astron. Astrophys. 583 (A43).

Mugrauer, M., 2024. Follow-up spectroscopy of comet C/2023 A3 (2024). In: The Astronomer's Telegram. 16911, p. 1.
Mumma, M.J., Charnley, S.B., 2011. The chemical composition of comets - emerging taxonomies and natal heritage. Annu. Rev. Astron. Astrophys. 49 (1), 471–524.
Rauer, H., et al., 2003. Long-term optical spectrophotometric monitoring of comet C/1995 O1 (Hale-Bopp). Astron. Astrophys. 397 (3), 1109–1122.
Russo, N.D., Hideyo, K., Ronald, Jr., V., Weaver, H.A., 2016. Emerging trends and a comet taxonomy based on the volatile chemistry measured in thirty comets with high-resolution infrared spectroscopy between 1997 and 2013. Icarus 278, 301–332.
Schleicher, D.G., 2009. The long-term decay in production rates following the extreme outburst of comet 17P/Holmes. Astron. J. 138 (4), 1062.
Tody, D., 1986. The IRAF data reduction and analysis system. In: Instrumentation in Astronomy VI. 627, SPIE, pp. 733–748.